East European Journal of Physics. 4. 537-544 (2024)
DOI:10.26565/2312-4334-2024-4-63 ISSN 2312-4334

FINITE ELEMENT ANALYSIS OF A DYNAMIC LINEAR CRACK PROBLEM

Brian E. Usibe[a]*, Williams E. Azogor[a], Prince C. Iwuji[a]*, Joseph Amajama[a], Nkoyo A. Nkang[b], Oruk O. Egbai[c], Alexander I. Ikeuba[d]

[a]*Department of Physics, University of Calabar, Nigeria*
[b]*Department of Science Laboratory Technology, University of Calabar, Nigeria*
[c]*Department of Environmental Resource Management, University of Calabar, Nigeria*
[d]*Materials Chemistry Research Group, Department of Pure and Applied Chemistry, University of Calabar, Nigeria*
**Corresponding Author e-mail: princechigozie42@yahoo.com; beusibe@unical.edu.ng*
Received July 14, 2024; revised October 20, 2024; in final form October 22, 2024; accepted October 30, 2024

This work investigates the problem of a linear crack in the middle of a uniform elastic medium under normal tension-compression loading. The direct Finite Element numerical procedure is used to solve the fractured media deformation problem, which also includes an examination of the dynamic field variables of the problem. A Finite Element algorithm that satisfies the unilateral Signorini contact constraint is also described for solving the crack faces' contact interaction, as well as how this affects the qualitative and quantitative numerical results while calculating the dynamic fracture parameter.
Keywords: *Harmonic loading; Linear crack; Fracture parameter; Contact interaction; Elastic medium; Finite Element Analysis*
PACS: 62.25.Mn

INTRODUCTION

Engineering materials are prone to cracking and delamination, which compromise the integrity of structures and components. The relationship between the load being applied and the dimension and location of a crack in an element can be determined using Fracture Mechanics solutions, which also help to predict the rate of crack formation and propagation [1, 2, 16]. As a result, it is vital to predict how fractured materials will react under dynamic loadings, as they are prone to failure under extremely small, unexpected loads. This is why it is critical to correctly determine the fracture parameter from the field variables, particularly as it is clear that under harmonic loading, the interior crack expands and contracts during the tension and compression phases, and the opposite crack faces move with respect to each other, significantly altering the stress and strain field near the crack tip [3, 4]. Until recently, the impacts of crack closure on fractured mechanics solutions were overlooked due to their level of complexity. However, it is extremely important to consider this phenomenon as the stresses and displacement jumps in cracked materials are usually higher for dynamic time-dependent conditions than in a static case, causing sudden failures in engineering structures even under small loads [5]. This is because the dynamic loading conditions induce more complex stress fields and crack propagation patterns than the static loading conditions.

The most important fracture parameter, the Dynamic Stress Intensity Factor (DSIF), which measures the intensity of the crack-tip stress field, is affected by the loading frequency, load direction and amplitude, material properties, and the crack dimension (shape and size). Therefore, the analysis of dynamic linear crack problems requires more advanced numerical methods and experimental techniques than the analysis of static linear crack problems [6]. Due to the complexity and non-linearity (even for LEFM conditions) presented by considering the dynamic effect of the problem [7], a numerical technique has been adopted for the solution, rather than using analytical methods that are limited to static solutions and simple crack configurations. As a result, the Finite Element numerical approach was employed in this study for obtaining the stress and displacement fields because it is reliable, convenient, and simple to calculate the appropriate fracture parameter [8-10]. The current method of Finite Element Analysis (FEA), which examines an in-plane linear crack situated in the centre of a homogeneous elastic medium, will provide knowledge of the dynamics of a cracked structural element under harmonic loading, as well as the computational determination of an essential fracture parameter, the dynamic Stress Intensity Factor (DSIF), which estimates an appropriate crack size and level of stress before crack propagation occurs. Finite Element Analysis (FEA) is a powerful numerical technique used to solve complex engineering problems, including analysing dynamic linear crack problems. Here, we refer to a dynamic linear crack problem as the study of how cracks propagate in a material when subjected to dynamic loading conditions. In the case of this study of a dynamic linear crack problem, the material is subjected to harmonic tension-compression incident pulse, causing the crack faces to move relative to each other. The Finite Element (FE) model of this study takes into account the material properties, the nature of applied loads, and the original centroid crack configuration. This information is critical in many science and engineering fields where structural health and integrity are important, including mechanical engineering, structural engineering, materials science, and physics. It aids in understanding failure mechanisms, enhancing material design, and forecasting the lifespan of engineered structures containing delamination and cracks. Because FEA is an approximation, its accuracy is determined by the mesh fineness, input data quality, and appropriate model assumptions. Despite some of

Cite as: B.E. Usibe, W.E. Azogor, P.C. Iwuji, J. Amajama, N.A. Nkang, O.O. Egbai, A.I. Ikeuba, East Eur. J. Phys. 4, 537 (2024), https://doi.org/10.26565/2312-4334-2024-4-63

its limitations, the FEA remains the most dependable technique for handling fracture mechanics problems that need dynamics analysis. It is crucial to highlight that under harmonic loading, both sides of the crack come into contact (during the compressive phase), which considerably changes the condition of the solution [11, 21 - 25]. In these works, the effects of crack closure were also examined, and the findings are provided in the following sections.

For the present study, the FE solution for the boundary value problem was implemented in the commercial software ABAQUS/CAE. The isoparametric hexahedral element was adapted for simulating the centroid crack. This choice was influenced by the fact that typical cracks are 3D in nature and the hexahedral elements satisfy the geometry of the fractured medium and the crack shape of the current study. The faces of the hexahedral elements align with the geometry and discontinuities of the discretized linear crack. The use of these hexahedral elements also makes it possible to accurately model the singularity of the crack front. The hexahedral isoparametric finite elements generally offer a solution with acceptable accuracy at a lower cost [18, 20]. It best describes the properties of this model as a three-dimensional continuous (solid) cube with explicit analysis (for dynamic stress and displacements) that allows for the modelling of various geometries and structures [16]. Mesh refinement and analysis of its sensitivity are used to determine the stress singularity. To satisfy the unilateral Signorini conditions, the "Hard contact" mechanical constraint was imposed in the Abaqus explicit solver.

THE PROBLEM DESCRIPTION

A harmonic incident wave with a unit amplitude of normal tension-compression load, propagating in a homogeneous elastic material is considered on the linear crack faces. Ideal elastic waves propagate through materials without causing a permanent change in their condition when the load is removed, but the material deforms and their cracked faces come into contact relative to each other, due to harmonic loading, as considered in this work.

This dissipation mechanism causes elastic waves to attenuate and scatter as they travel, and the rate of attenuation is usually proportional to the incident wave's frequency [12, 13].

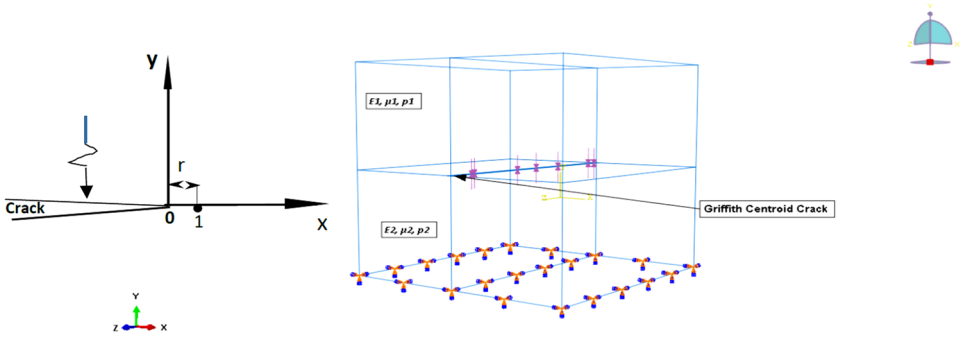

Figure 1. (a) - Crack geometry, (b) - FE Model of linear crack under normal tensile-compressive loading

The homogeneous material is composed of two half-spaces with identical material properties. The linear crack is located at the center of the domain. The solid domain ($\Omega_1 = \Omega_2$) with both lower and the upper half-spaces ($E_1 = E_2$, $\nu_1 = \nu_2$, $\rho_1 = \rho_2$) has the following properties of steel [The Young's modulus (E) = 200 GPa, The Poisson's ratio (ν) = 0.3, density (ρ) = 7800 kg/m^3], and we assume that only small deformations occur according to LEFM. Figure 1 shows the 3D model built with Abaqus/CAE with an initial non-zero crack opening of $h_0 = 10^{-6}$mm in a Cartesian coordinate system, such that the path of the incident wave is at right angles to the interface. The incident wave was applied at frequencies and corresponding wavenumbers of $k_\alpha = 0.1$ and the normal angle of the wave incidence, $\theta_0 = 0^0$.

The interface separating the half-spaces, Γ^*, serves as the boundary for the top half-space, Γ^1, while the bottom half-space is represented by Γ^2. In this model case, surfaces 1 and 2 consist of a finite part (crack surface) with a specific dimension and crack size ($2a$), and the bonding interface; all of which satisfies the plane strain condition. The crack surface for materials 1 and 2 is represented by Γ^{cr} such that;

$$\Gamma cr = \Gamma^{1(\mathrm{Cr})} \cup \Gamma^{2(\mathrm{Cr})} \tag{1}$$

The spatial distribution of tractions at the point of bonding, $\Gamma^* = \Gamma^{1(Cr)} \cap \Gamma^{2(Cr)}$, meets the continuity criteria for displacements and stresses, so that;

$$U^1(x,t) = -U^2(x,t), P^1(x,t) = -P^2(x,t) \{x \in \Gamma^*, \mathrm{t} \in \mathrm{T}\} \tag{2}$$

The unknown traction vectors on the crack's surfaces induced by the external loads are:

$$p^1(x,t) = -g^1, \{x \in \Gamma^{1(Cr)}, \mathrm{t} \in \mathrm{T}\}$$

$$p^2(x,t) = g^2, \{x \in \Gamma^{2(Cr)}, \mathrm{t} \in \mathrm{T}\} \tag{3}$$

Where (x, t) is the displacement vector, $p(x, t)$ is the traction vector, and $g(x, t)$ is the load caused from the incoming wave [3, 9].

The traction vector, (x, t), on each face of the fracture is given by:

$$(x, t) = g(x, t) + q(x, t) \tag{4}$$

The vector (x, t) represents the contact force at the contact area (Γ^{cr}).

The "small" initial crack opening introduced in the model problem of this work satisfies the condition of non-zero initial opening. Signorini constraints must be imposed for the normal components of the contact force and the displacement discontinuity vectors [13-15]. The constraints ensure that there is no interpenetration of the opposite crack faces and there are no initial contact forces due to a non-zero initial opening of the crack. The constraints are given by the following inequalities;

$$\Delta u_n\,(x,t) \geq -h_0(x)\,;\, h_0(x) > 0, \tag{5}$$

$$q_n(x,t) \geq 0,$$

$$\therefore\ (\Delta u_n\,(x,t) + h_0(x))\, q_n(x,t) = 0. \tag{6}$$

Where h_0 is the initial crack initial opening:

$$h_0 = b\Delta u^{stat,\ max} a\,(1 + \cos\,(\pi\sqrt{x_1^2 + x_2^2}/a))\,/2 \tag{7}$$

The maximum crack opening under static normal loading is represented by $\Delta u^{stat,\ max} = 2(1-\nu)/\mu$, while b represents the normalized magnitude of the crack's initial opening [13].

Dynamic Stress Distribution in Elastic Homogeneous Material

The magnitude of the applied load is defined with a step time using the Fourier function;

$$f(t) = a_0 + \sum_{n=1}^{\infty}(A_n \cos\omega t + B_n \sin\omega t) \tag{8}$$

The amplitudes A_n and B_n of the Fourier functions are depicted by the elements of the tractions and displacements, respectively, as illustrated below:

$$p_{cos}\,(x) = \frac{\omega}{2\pi}\int_0^T p\,(x,t)\ \cos(\omega t)\,dt\ ,\ u_{cos}\,(x) = \frac{\omega}{2\pi}\int_0^T u\,(x,t)\ \cos(\omega t)\,dt \tag{9}$$

$$p_{sin}\,(x) = \frac{\omega}{2\pi}\int_0^T p\,(x,t)\ \sin(\omega t)\,dt\ ,\ u_{sin}\,(x) = \frac{\omega}{2\pi}\int_0^T u\,(x,t)\ \sin(\omega t)\,dt. \tag{10}$$

The potential function defines the incident tension-compression harmonic wave as:

$$\Phi\,(x,t)\ = \Phi_0 e^{i(k_\alpha x_n - \omega t)} \tag{11}$$

In Figure 2, Φ_0 and ω represent the amplitude and circular frequency (ω = 2πf) of the incident wave, respectively. k_α is the generalized wave number given by $k_\alpha = {}^{\omega}/_{C\alpha}$ and C_α are the velocities of incident waves in isotropic elastic media [3,11,13].

$$C_1 = \sqrt{\frac{\lambda+2\mu}{\rho}}\ \text{(Longitudinal wave)},\ C_2 = \sqrt{\frac{\mu}{\rho}}\ \text{(Transverse wave)}. \tag{12}$$

Where λ and μ are lame constants, and ρ is the density of the material (steel). Figure 2 depicts the unit amplitude of the incident sine wave (equation 10) travelling as a function of time, t, along the normal y-direction (x_2 axis), with tensile (crest) and compressive (trough) phases.

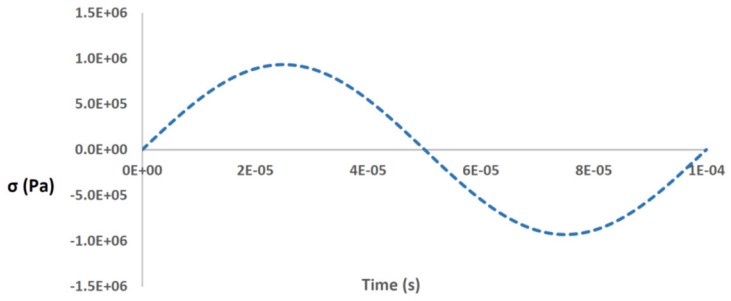

Figure 2. Harmonic incident wave pattern

The applied load of 1 MPa is a time-dependent sinusoidal incident wave, and at a given frequency, the generalized wave number (k_α) is obtained and the corresponding dynamic field variable is then extracted. Since the two half-spaces are made of the same materials, there is no change in the properties of the wave distribution between them. The incident wave is completely transmitted into lower material and there is no reflection. The initial incident wave propagates through both half-spaces with the magnitude of reflected and transmitted waves equal to zero. Section 5 of this work describes the distribution of the normal components of the dynamic field variables.

Finite Element Approximation

The appropriate Finite Element approximation for the linear interface crack is based on those obtained in [16] and briefly described in Section 1 of this study. Again, to establish the presence of stress singularities at the crack tip only requires a mesh refinement around that region of interest. This enables the accurate assessment of reliable field variables at the crack tip.

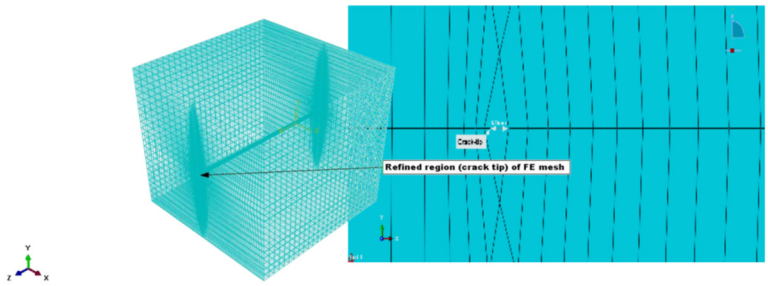

Figure 3. FE mesh discretization for the Griffith crack

In this Finite Element composition, no specific crack tip elements were required. Mesh refinement and sensitivity analysis were adequate to approximate the singularity condition at the crack tip of the FE model. Figure 4 depicts the numerical GUI results of the FE model. When the harmonic load is applied, under compression, the stress level at the contact region of the crack surfaces increases, and the model deforms depending on the load increment, with each successive step until the entire process is completed [16].

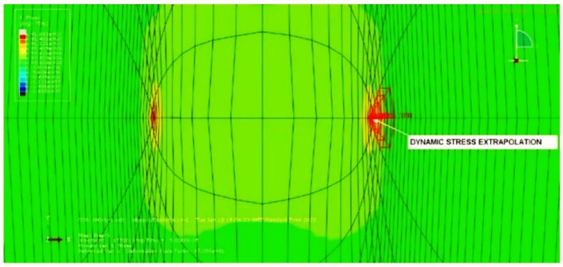

Figure 4. FE model with Stress Extrapolation

NUMERICAL RESULTS AND DISCUSSIONS

In this study, the numerical distribution of the stress field variables is extracted at the points of integration nearest to the crack tip, whereas displacements are determined at relative nodal points indicating the vicinity of the tip [16-18]. Note that $r = 0$ is the crack tip with infinite stresses (which is not realistic in real materials). Away from the crack tip, field variables become less valuable for fracture parametric analysis. Therefore, the region under consideration must be as close to the tip as possible ($0 < r/a \leq 1$) [19, 20] to obtain accurate results with desired stability and reduced distortion of the elements around the crack-tip region. To model this "small" distance from the crack tip, the meshing "art" becomes very useful. Another way to avoid infinite stresses is to assume some elastic deformation during loading in order to provide a large area during the contact of crack faces.

The desired stresses are in the y-direction of the tension-compression load, and they are extracted at the Integrating Points in the FE model and then extrapolated to nodal points to represent the crack tip, for evaluation. This also gives a good approximation of stress singularity.

The distribution of the normal component of the harmonic stress waves along the crack plane during the entire period of oscillation ($0 \leq \omega t \leq 2\pi$) for wave number $k_\alpha = 0.1$ is shown in Figure 5. It shows that the stresses rapidly decrease with distance from the crack front and vice versa.

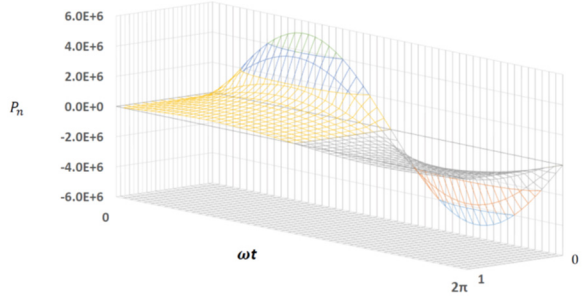

Figure 5. Normal distribution of stresses near the crack front

On the other hand, the magnitudes of normal displacement discontinuities along the diametrical crack surface before and after loading are presented in Figure 6. The normal distribution of displacement of the crack surfaces during the oscillation period ($0 \leq \omega t \leq 2\pi$) for wave number $k_\alpha = 0.1$ is also presented in Figure 7 for the leading edge of the crack. In the current study, there is symmetry between the leading (+) and trailing (-) crack fronts (see Figure 6), so only one front (the leading) of the specimen is used for the analysis.

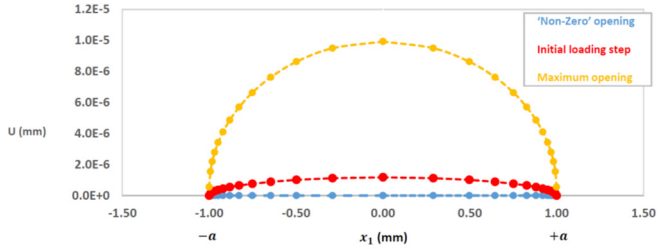

Figure 6. Magnitude of normal displacements along the diametrical crack face before and after loading (upper half-space)

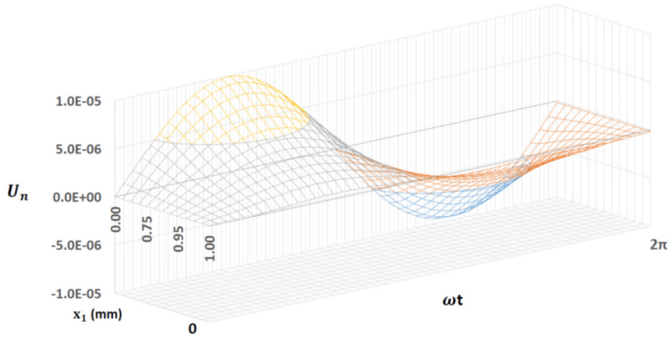

Figure 7. Normal distribution of displacement discontinuity without contacts interaction (upper half-space)

It should be noted that the tangential components of the stresses and displacements are absent or negligible due to the location of the crack in relation to the direction of the loading and the small curvature of the crack faces. Therefore, it was only necessary to evaluate the normal components of the solution.

There are no contact forces during the tensile phase of harmonic loading and crack opening, as shown in Figure 8. However, when unilateral constraints are enforced, the contact forces become present (see section 6 below).

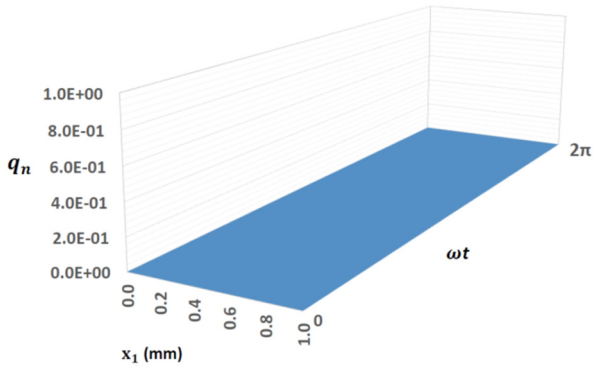

Figure 8. Absence of contact forces at the crack surface due to the opening of the crack faces

Finite Element Algorithm for Contact Interaction

Following the solution of the current problem, the Finite Element contact interaction has been implemented with the algorithm below for the next stage of this study.

1. Apply initial harmonic loads, which completes the description of the physical problem
2. Solve for Fourier coefficients using equations (8) to (10)
3. Obtain the initial stresses and displacements without contact constraints
4. Define interaction pair for the crack (contact surfaces) without friction ($\hbar = 0$)
5. Apply Kinematic contact conditions to satisfy Signorini constraints of equations (5) and (6)
6. Check for overlapping and penetration of crack surfaces; if yes, then go to 5 and repeat
7. Else, go to 8
8. Obtain the unknown stresses and displacements of interest under contact

9. Obtain unknown contact forces resulting from 5 and as part of 8
10. Repeat the algorithm to get all the appropriate extrapolated variables at the crack tip
11. Extract the numerical results and post-process using an IDE
12. Compute the Dynamic Stress Intensity Factors from 3, 8 and 11 without and with contact interaction

Figure 9 shows the linear crack under contact constraints. When external forces or pressures cause the crack surfaces to interact or remain in contact, it is said to be a linear crack under contact constraints. This situation often occurs in materials where the behavior and transmission of the crack are influenced by friction, crack closure or other boundary conditions.

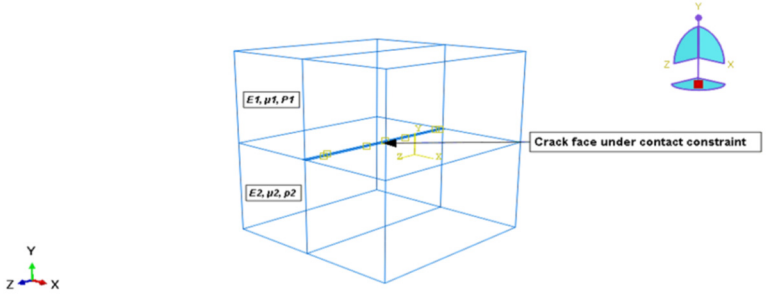

Figure 9. FE Model of Linear crack under contact constraints

In Figure 9, the constraints shown in the middle of the model (with yellow dentations) are the contact interaction properties that are imposed as boundary conditions on the crack faces of the FE model to address the components of the contact forces and load vector on the crack surfaces as indicated in equations (5) through (7). Using isoparametric surface-to-surface contact discretization and a "Hard" Kinematic mechanical constraint method from [19], the Signorini contact conditions are strictly enforced, and the penetration of contact elements is minimized. The numerical results are extracted without and with the effects of the crack closure.

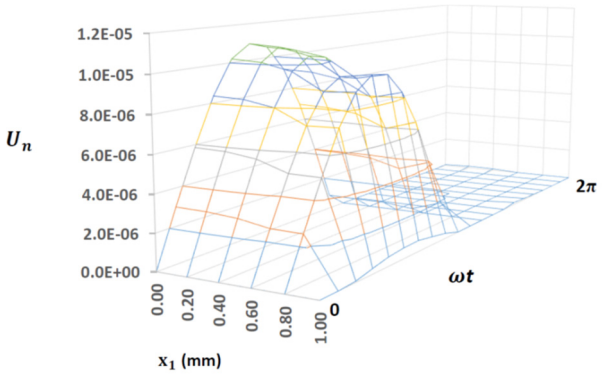

Figure 10. Distribution of normal displacement considering contact interaction

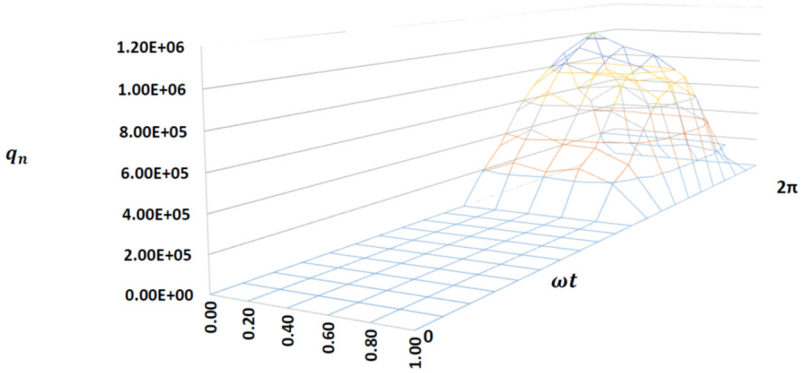

Figure 11. Normal contact forces at the crack surface

Figures 10 and 11 show the normal distribution of displacement and the corresponding contact force at the crack face during the period of oscillation ($0 \leq \omega t \leq 2\pi$) for wavenumber $k_\alpha = 0.1$ for the upper half-space at the leading edge of the crack. It is shown that the distribution of the normal component of the displacement, even during the tensile phase is significantly altered when the contact interaction of the opposite crack faces is considered (see line 5 of the algorithm). The kinematic contact constraints enforced during the period of oscillation prevent the interpenetration (overclosure) of the crack faces. The displacement discontinuity over the crack surface is observed to be distorted, especially during the

compressive phase where contact takes place. By the elimination of the interpenetration of the contacting (crack) surfaces, there is a corresponding contact force which repels the slave surfaces from the master sections, thereby leading to a substantial decrease in the magnitude of the normal component of the displacement discontinuity (see line 6 of the algorithm). This accounts for the qualitative and quantitative changes in determining the fracture parameter, Stress Intensity Factors (SIF) without and with contact interactions.

Using the asymptotic expression from [21], the Stress Intensity Factors for mode I is determined as the next stage of this study as follows:

$$K_I = \lim_{r\to 0} \sigma_y \sqrt{2\pi r} \tag{13}$$

Where r is the distance from the crack front. In this problem, there is symmetry between the leading (+) and trailing (-) crack fronts (see Figure 6), so only one front of the specimen would be used for the determination of the mode I fracture parameter and the values of the Stress Intensity Factors would be normalized by the static value, and the results validated with those from [22, 26].

$$K_I^{stat} = \sigma_y \sqrt{\pi a} \tag{14}$$

From equations (13) and (14), and by the stress extrapolation method shown in Figure 4, the Dynamic Stress Intensity Factor at the crack front can be determined, neglecting, and taking the effects of contact interaction into account.

CONCLUSIONS

The direct Finite Element Analysis was used to obtain the normal opening mode of dynamic stresses at the crack tip, and the displacements across the diametrical crack face of a homogeneous fractured media. The normal (Mode I) distribution of stresses along the crack plane during the entire period of oscillation ($0 \leq \omega t \leq 2\pi$) for wave number $k_\alpha = 0.1$ was determined and analyzed. The magnitudes of normal displacements along the diametrical crack face before and after loading were also analyzed for the upper half-space with a distribution of displacement (without and with contact interaction) of the crack faces during the period of oscillation. The dynamic numerical results show that the nature of dynamic loading and the frequency of the incident wave on the cracked elastic media affect the distribution of the stress waves and therefore alter the fracture parameter significantly.

In what follows the solution of the current problem; the implemented Finite Element algorithm satisfies the unilateral Signorini constraints for the contact interaction on the surface of the crack during the period of oscillation and leads to the determination of the dynamic Stress Intensity Factor for varying (higher) wave numbers.

Funding: This study received no external funding.
Conflict of Interest: There are no conflicts of interest.

ORCID

Brian E. Usibe, https://orcid.org/0000-0003-4388-2480; **Prince C. Iwuji,** https://orcid.org/0000-0001-5715-9336
Joseph Amajama, https://orcid.org/0000-0002-8475-9457; **Alexander I. Ikeuba,** https://orcid.org/0000-0001-5091-8651

REFERENCES

[1] A.A. Griffith, "The phenomena of rupture and flow in solids," Philosophical Transactions of the Royal Society of London, Series A, **221**, 163-198 (1921).
[2] T.L. Anderson, *Fracture Mechanics. Fundamentals and Applications*," 2nd edition, (CRC Press, Boca Raton, 1995).
[3] O.V. Menshykov, and I.A. Guz, "Effect of Contact Interaction of the Crack Faces for a Crack under Harmonic Loading," International Applied Mechanics, **43**, 809-815 (2007). https://doi.org/10.1007/s10778-007-0082-y
[4] A.N. Guz, and V.V. Zozulya, "Contact interaction between crack edges under a dynamic load," Int. Appl. Mech," **28**, 407–414 (1992). https://doi.org/10.1007/BF00847122
[5] L. Zhang, Z. Zhang, Y. Chen, B. Dai, and B. Wang, "Crack development and damage patterns under combined dynamic-static loading of parallel double fractured rocks based on DIC technique," Acta Geotech, **18**, 877–901 (2023). https://doi.org/10.1007/s11440-022-01595-5
[6] S. Abu-Qbeitah, M. Jabareen, and K. Y. Volokh, "Dynamic Versus Quasi-Static Analysis of Crack Propagation in Soft Materials," ASME. J. Appl. Mech. **89**, 121008 (2022). https://doi.org/10.1115/1.4055670
[7] P. Wriggers, "Finite Element Algorithms for Contact Problems. Archives of Computational Methods in Engineering," State-of-the-art reviews, **2**, 1–49 (1995). https://doi.org/10.1007/BF02736195
[8] M. Schäfer, *Computational Engineering – Introduction to Numerical Methods*, (Springer Berlin Heidelberg, New York, 2006).
[9] K.H. Huebner, D.L. Dewhirst, D.E. Smith, and J.G. Byron, *The Finite Element for Engineers*, (Wiley-interscience, New York, 2001).
[10] Q. Han, Y. Wang, Y. Yin, and D. Wang, "Determination of stress intensity factor for mode I fatigue crack based on finite element analysis," Engineering Fracture Mechanics, **138**, 118–126 (2015). https://doi.org/10.1016/j.engfracmech.2015.02.019
[11] O.V. Menshykov, M.V. Menshykova, I.A. Guz, and V.A. Mikucka, "Contact Problems for Interface Cracks under Harmonic Loading," Appl. Math. **10**, 127–128 (2010). https://doi.org/10.1002/pamm.201010056
[12] S.M. Walley, and J.E. Field, *Elastic Wave Propagation in Materials*, (Cavendish Laboratory, Cambridge, UK, 2016). https://doi.org/10.1016/B978-0-12-803581-8.02945-3

[13] O.V. Menshykov, V.A. Menshykov, and I.A. Guz, "The contact problem for an open penny-shaped crack under normally incident tension-compression wave," Engineering Fracture Mechanic, **75**, 1114–1126 (2008). https://doi.org/10.1016/j.engfracmech.2007.04.017
[14] M.V. Menshykova, O.V. Menshykov, and I.A. Guz, "Modelling crack closure for an interface crack under harmonic loading," Int. J. Fracture, **165**, 127–134 (2010). https://doi.org/10.1007/s10704-010-9492-7
[15] M.V. Menshykova, O.V. Menshykov, V.A. Mikucka, and I.A. Guz, "Interface cracks with initial opening under harmonic loading," Composites Science and Technology, **72**, 1057-1063 (2012). https://doi.org/10.1016/j.compscitech.2011.10.010
[16] B.E. Usibe, and O.V. Menshykov, "Evaluation of Dynamic Stress Intensity Factor of Griffith Crack Using the Finite Element Method," International Journal of Mechanics and Applications, **10**, 1-10 (2021). https://doi.org/10.5923/j.mechanics.20211001.01
[17] S.K. Chan, L.S. Tuba, and W.K. Wilson, "On the Finite Element Method in Linear Fracture Mechanics," Engineering Fracture Mechanics, **2**, 1-17 (1970). https://doi.org/10.1016/0013-7944(70)90026-3
[18] B. Zafošnik, and G. Fajdiga, "Determining Stress Intensity Factor K_I with Extrapolation Method," Technical Gazette, **23**, 1673-1678 (2016). http://dx.doi.org/10.17559/TV-20150424160509
[19] ABAQUS/CAE User's Manual, Version 6.14-1
[20] C. Obbink-Huizer, *Modelling a crack using Abaqus: Simuleon FEA*, Accessed 16 December 2022. https://info.simuleon.com/blog/modelling-a-crack-using-abaqus
[21] D. Gross, and T. Seelig, *Fracture Mechanics with an Introduction to Micromechanics*, (Springer Heidelberg Dordrecht, New York, 2011).
[22] A.N. Guz, and V.V. Zozulya, "Elastodynamic unilateral contact problems with friction for bodies with cracks," International Applied Mechanics, **38**, 895–932 (2002). https://doi.org/10.1023/A:1021266113662
[23] O.V. Menshykov, M.V. Menshykova, and I.A. Guz, "3-D elastodynamic contact problem for an interface crack under harmonic loading," Engineering Fracture Mechanics, **80**, 52– 59 (2012). https://doi.org/10.1016/j.engfracmech.2010.12.010
[24] O.V. Menshykov, M.V. Menshykova, and I.A. Guz, "Effects of crack closure and friction for linear crack under normal impact," Eng. Anal. Bound. Elem. **115**, 1–9 (2020). https://doi.org/10.1016/j.enganabound.2020.02.013
[25] O.V. Menshykov, V.A. Menshykov, and I.A. Guz, "The effect of frequency in the problem of interface crack under harmonic loading," Int. J. Fract. **146**, 197-202 (2007). https://doi.org/10.1007/s10704-007-9157-3
[26] V.A. Mikucka, O.V. Menshykov, and M.V. Menshykova, "Elastodynamic Contact Problems for Interface Cracks under Harmonic Loading," Proceedings in Applied Mathematics and Mechanics, **11**, 165-166 (2011). https://doi.org/10.1002/pamm.201110074

КІНЦЕВО-ЕЛЕМЕНТНИЙ АНАЛІЗ ПРОБЛЕМИ ДИНАМІКИ ЛІНІЙНОЇ ТРІЩИНИ

Брайан Е. Усібе[a], Вільямс Е. Азогор[a], Принц Ч. Івудзі[a], Джозеф Амаджама[a], Нкойо А. Нканг[b], Орук О. Егбай[c], Олександр І. Ікеуба[d]

[a]Департамент фізики, Університет Калабара, Нігерія
[b]Департамент наукових лабораторних технологій, Університет Калабара, Нігерія
[c]Департамент управління екологічними ресурсами, Університет Калабара, Нігерія
[d]Дослідницька група з хімії матеріалів, Департамент чистої та прикладної хімії, Університет Калабара, Нігерія

У роботі досліджено задачу про лінійну тріщину в середині однорідного пружного середовища при нормальному навантаженні розтяг-стискування. Пряма чисельна процедура кінцевих елементів використовується для розв'язання задачі деформації середовища з тріщинами, яка також включає дослідження змінних динамічного поля задачі. Алгоритм кінцевих елементів, який задовольняє одностороннє контактне обмеження Синьоріні, також описано для вирішення контактної взаємодії поверхонь тріщин, а також як це впливає на якісні та кількісні числові результати під час розрахунку динамічного параметра руйнування.

Ключові слова: *гармонічне навантаження; лінійна тріщина; параметр руйнування; контактна взаємодія; еластичний середній; кінцево-елементний аналіз*